

Wave simulation in dissipative media described by distributed-order fractional time derivatives

Michele Caputo^{1,2} and José M Carcione³

Journal of Vibration and Control
17(8) 1121–1130
© The Author(s) 2010
Reprints and permissions:
sagepub.co.uk/journalsPermissions.nav
DOI: 10.1177/1077546310368697
jvc.sagepub.com



Abstract

We develop and solve a dissipative model for the propagation and attenuation of two-dimensional dilatational waves, using a new modeling algorithm based on distributed-order fractional time derivatives. We consider two distributions. The first has n powers of the order of differentiation as the weight function, and the second is based on a generalized Dirac's comb function. The wave equation is solved with the fractional derivative by means of a generalization of the Grünwald–Letnikov approximation. The modeling uses the Fourier method to compute the spatial derivatives, and therefore can handle complex geometries and general material-property variability. We verify the results by comparison with the two-dimensional analytical solution obtained for wave propagation in homogeneous media. Moreover, we illustrate the use of the modeling algorithm by simulating waves in the presence of an interface separating two dissimilar media.

Keywords

Anelasticity, distributed order, fractional derivatives, waves, dissipation

Received: 14 December 2009; accepted: 9 March 2010

1. Introduction

Stress–strain relations based on fractional derivatives provide a suitable model of seismic attenuation in attenuating media. Caputo (1967), Caputo and Mainardi (1971), Carcione et al. (2002) and Carcione (2009) described the anelastic behavior of general materials over wide frequency ranges by using fractional derivatives, in particular considering propagation with constant- Q characteristics. Bland (1960) and Kjartansson (1979) discuss such a linear attenuation model, but the idea is much older (Scott-Blair, 1949). Mainardi and Tomirotti (1997) interpreted the constant- Q model in terms of fractional derivatives and obtained its one-dimensional Green's function based on the Mittag-Leffler function. A hyperbolic power law that can also be implemented using fractional derivatives has been introduced by Hanyga and Sereďyńska (2003), who discuss the causal properties associated with the model of Kjartansson (1979). The governing equation becomes parabolic since the phase velocity as a function of frequency has no upper bound.

The case of two-dimensional compressional (P)-wave propagation in heterogeneous media has been solved by Carcione et al. (2002). Instead of time derivatives of order two, they used derivatives of order $2 - q$ with $0 < q < 1$ in the dilatation formulation of the wave equation, and order q in the dilatation–stress formulation. The case of two-dimensional propagation of P and shear (S) waves has been developed and solved numerically by Carcione (2009). Here, we extend the theory and the algorithm to model the propagation and attenuation of P waves, where the stress–strain relation is described by distributed-order fractional

¹Department of Physics, University “La Sapienza”, Rome, Italy

²Department of Geology and Geophysics, Texas A & M University, College Station, TX, USA

³Istituto Nazionale di Oceanografia e di Geofisica Sperimentale (OGS), Sgonico, Trieste, Italy

Corresponding author:

José M Carcione, Istituto Nazionale di Oceanografia e di Geofisica Sperimentale (OGS), Sgonico, Trieste, Italy
Email: jcarcione@inogs.it

derivatives, i.e. the derivatives are integrated with respect to the order of differentiation. Compared with the single-derivative case, this generalization introduces one more parameter and allows us to model more general variations of the phase velocity and quality factor as a function of frequency. The idea has already been described by Caputo (1967) and further developed in Caputo (1995, 2001). Mainardi et al. (2007, 2008) discuss the fractional diffusion of double order and of uniformly distributed order and obtain the fundamental solutions in terms of the Mittag-Leffler functions. Fractional differential equations consisting of sums of fractional-order derivatives have been extensively studied by Podlubny (1999). Here, we consider a continuum spectrum of orders based on n powers of the order of differentiation and a discrete distribution based on Dirac's comb function.

Fractional derivatives can be computed with the Grünwald–Letnikov (GL) approximation (Grünwald, 1867; Letnikov, 1868; Caputo, 1967), which is an extension of the standard finite-difference (FD) approximation for derivatives of integer order (Grünwald, 1867; Letnikov, 1868; Gorenflo, 1997). Unlike the standard operator of differentiation, the fractional operator increases in length as time increases, since it must keep the memory effects. However, after a given time period the operator can be truncated (short memory principle). The presence of the distributed-order derivatives requires the generalization of the GL approximation.

In the first part of this work we introduce the stress–strain relation and calculate the complex moduli, phase velocities, and attenuation and quality factors versus frequency. We then recast the wave equation in the time-domain in terms of fractional derivatives and obtain the GL approximation. Then, we verify the accuracy of the time discretization by comparing the exact and the FD phase velocities and attenuation factors. The model is discretized on a mesh, and the spatial derivatives are calculated with the Fourier method by using the fast Fourier transform (FFT). This approximation is infinitely accurate for band-limited periodic functions with cutoff spatial wavenumbers smaller than the cutoff wavenumbers of the mesh. Finally, we test the modeling algorithm with an analytical solution for a two-dimensional homogeneous medium, and illustrate the method with a numerical simulation in inhomogeneous media.

2. The stress–strain relation for a single derivative

Caputo (1967), Caputo and Mainardi (1971), Carcione et al. (2002) and Carcione (2009) described and computed the anelastic behavior of many materials over

wide frequency ranges by using fractional derivatives. The corresponding stress (σ)–strain (ϵ) relation for a given deformation is

$$\sigma = M \frac{\partial^q \epsilon}{\partial t^q}, \quad 0 \leq q \leq 1, \quad (1)$$

where M is a pseudo-stiffness, which is a stiffness for $q=0$ and a viscosity for $q=1$. The limits $q=0$ and $q=1$ give Hooke's law and the constitutive relation of a dashpot (Carcione, 2007).

In the frequency domain, we obtain

$$\sigma = \bar{M} \epsilon, \quad (2)$$

where

$$\bar{M} = M p^q, \quad p = i\omega \quad (3)$$

is the complex stiffness, with ω the angular frequency. We may write,

$$M = M_0 \omega_0^{-q} \quad (4)$$

(Carcione, 2009), where ω_0 is a reference frequency. Then,

$$\bar{M} = M_0 \left(\frac{i\omega}{\omega_0} \right)^q, \quad (5)$$

Note that M has the units [Pa s ^{q}]. The complex modulus (equation 5) vanishes at zero angular frequency, thus the quasi-static elastic limit is not represented by this model. Hence, applications should be restricted to band-limited sources with a nonzero dominant frequency.

The quality factor Q quantifies the amount of dissipated energy. It is defined as $Q = \text{Re}(v^2)/\text{Im}(v^2)$ (e.g. Carcione (2007, equation 2.120)), where $v^2 = [M(i\omega/\omega_0)^q]/\rho$, with v the complex velocity, ρ the mass density, and “Re” and “Im” denote real and imaginary parts, respectively. We obtain

$$Q = \frac{1}{\tan(\pi q/2)}, \quad (6)$$

which is constant (independent of frequency). If Q is infinite there is no dissipation ($q=0$).

3. The stress–strain relation for distributed orders of derivatives

The stress–strain relation (equation 1) is generalized to the case when the fractional-order derivatives are

integrated with respect to the order of differentiation, i.e. we consider a spectrum of derivatives,

$$\sigma = M_0 \int_a^b s(z) \frac{\partial^z \epsilon}{\partial t^z} dz \tag{7}$$

(Caputo, 1967, 2001), where $0 \leq a \leq b \leq 1$ and $s(z)$ is the distribution of the derivatives. If $s(z) = \delta(z - q)$, we obtain equation 1. The introduction of one more parameter (a and b instead of z) renders the stress-strain relation more flexible because it includes a variety of memory mechanisms and is more apt to represent the dispersion acting with several different relaxations (e.g. anelastic relaxation mechanisms or spectral lines in the case of dielectric media). We consider two main cases, namely the case $s(z) = z^n$ and a generalized Dirac's comb function. In the first case, a continuous spectrum can be represented, while the second distribution may describe a physical process with well-defined wave-like and diffusion-like behavior depending on the discrete values assumed.

3.1. The z^n Case

We assume

$$s(z) = N \omega_0^{-z} z^n, \quad N = \frac{n+1}{b^{n+1} - a^{n+1}}, \tag{8}$$

where n is a natural number and N is a normalization constant such that $\omega_0^{-z} \int_a^b s(z) dz = 1$. The quantity ω_0^{-z} is included to avoid powers of p (or of ω) having different dimensions, which would be physically unacceptable (see equation 4). The frequency-domain version of equation 7 is

$$\sigma = M_0 \epsilon \int_a^b s(z) p^z dz = M_0 \epsilon \int_a^b N z^n u^z dz = \bar{M} \epsilon, \tag{9}$$

$$u = \omega_0^{-1} p = \frac{i\omega}{\omega_0}, \tag{10}$$

$$\bar{M} = M_0 S, \tag{11}$$

and

$$S(u) = \int_a^b N z^n u^z dz. \tag{12}$$

Here S is dimensionless and M_0 is in units of Pa.

Using the property $u^z = \exp(z \ln u)$ and an indefinite integral for the exponential function, we obtain

$$S(u) = N \sum_{k=0}^n \frac{(-1)^k k!}{(\ln u)^{k+1}} \binom{n}{k} (u^b b^{n-k} - u^a a^{n-k}). \tag{13}$$

The case $n=0$ gives

$$S(u) = \frac{N}{\ln u} (u^b - u^a), \quad N = \frac{1}{b-a}, \tag{14}$$

and the case $n=1$ gives

$$S(u) = \frac{N}{\ln u} \left[\left(b - \frac{1}{\ln u} \right) u^b - \left(a - \frac{1}{\ln u} \right) u^a \right], \tag{15}$$

$$N = \frac{2}{b^2 - a^2}.$$

In the first case, all of the derivatives have the same weight (uniform distribution).

3.2. The Generalized Dirac's Comb Function

We define a generalized Dirac's comb function, where the delta functions are not equally spaced and each one has a different weight,

$$s(z) = \omega_0^{-z} \sum_{k=1}^n a_k \delta(z - z_k), \tag{16}$$

where a_k are the weights satisfying $\sum_{k=1}^n a_k = 1$, and $a \leq z_k \leq b$. Then

$$S(u) = \int_a^b \sum_{k=1}^n a_k \delta(z - z_k) u^z dz, \tag{17}$$

which simplifies to

$$S(u) = \sum_{k=1}^n a_k u^{z_k}. \tag{18}$$

4. Kinematics and energy balance

This analysis yields the measurable quantities, such as the phase velocity, and the attenuation and quality factors.

4.1. Complex velocity, Phase Velocity and Attenuation Factor

As above, we define the complex velocity as

$$v = \sqrt{\frac{\bar{M}}{\rho}} = \sqrt{\frac{M_0 S}{\rho}}. \tag{19}$$

Then, the phase velocity and attenuation factor are obtained from the complex velocity as

$$v_p = [\text{Re}(v^{-1})]^{-1} \quad \text{and} \quad \alpha = -\omega \text{Im}(v^{-1}) \tag{20}$$

(Carcione, 2007), respectively, where equation 11 has been used.

4.2. Quality Factor

The Umov–Poynting theorem or energy balance equation for harmonic fields in anelastic media is given by

$$\operatorname{div} \cdot \mathbf{p} - i\omega(V - K) + D = 0 \quad (21)$$

(e.g. Carcione (2007, equation 4.57)), where \mathbf{p} is the complex power-flux vector, V is the strain (stored) energy, K is the kinetic energy and D is the dissipated energy. These are energy densities, i.e. time-averaged energies in one cycle per unit volume.

The time-averaged strain energy density per cycle is given by

$$V = \frac{1}{4} \operatorname{Re}(\bar{M})|\epsilon|^2 \quad (22)$$

(see Carcione (2007, equation 2.104)). For $\epsilon = \epsilon_0 \exp(pt)$, we have

$$V = \frac{1}{4} \operatorname{Re}(\bar{M})|\epsilon_0|^2 = \frac{1}{4} M_0 \operatorname{Re}(S)|\epsilon_0|^2. \quad (23)$$

The time-averaged dissipated energy density per cycle is given by

$$D = \frac{1}{2} \operatorname{Im}(\bar{M})|\epsilon|^2 \quad (24)$$

(see Carcione (2007, equations 2.105, 4.85 and 4.114)). For $\epsilon = \epsilon_0 \exp(pt)$, we have

$$D = \frac{1}{2} \operatorname{Im}(\bar{M})|\epsilon_0|^2 = \frac{1}{2} M_0 \operatorname{Im}(S)|\epsilon_0|^2. \quad (25)$$

The quality factor is defined as

$$Q = \frac{2V}{D} = \frac{\operatorname{Re}(\bar{M})}{\operatorname{Im}(\bar{M})} = \frac{\operatorname{Re}(S)}{\operatorname{Im}(S)}, \quad (26)$$

according to equation 11.

In isotropic media, the energy velocity, defined as the power-flux vector $\operatorname{Re}(\mathbf{p})$ divided by the total energy $V + K$, is equal to the phase velocity (Carcione, 2007).

5. Two-dimensional dynamical equations

The conservation of linear momentum for a two-dimensional linear anelastic medium, describing dilatational deformations, can be written as

$$\rho \partial_t^2 u_i = \partial_i \sigma, \quad i = 1(x), 2(y) \quad (27)$$

(Auld, 1991; Carcione, 2007), where u_i are the components of the displacement vector and ∂_i computes the spatial derivative with respect to x_i . The initial conditions are $u_i(0, \mathbf{x}) = 0$, $\partial_t u_i(0, \mathbf{x}) = 0$, and $u_i(t, \mathbf{x}) = 0$, for $t < 0$, where \mathbf{x} is the position vector. The strain–displacement relation is $\epsilon = \partial_1 u_1 + \partial_2 u_2$. Then, the complete set of equations describing the propagation is

$$\begin{aligned} \partial_t^2 u_1 &= \rho^{-1} \partial_1 \sigma, \\ \partial_t^2 u_2 &= \rho^{-1} \partial_2 \sigma, \\ \sigma &= M_0 \int_a^b s(z) \frac{\partial^z \epsilon}{\partial t^z} dz + s, \\ \epsilon &= \partial_1 u_1 + \partial_2 u_2, \end{aligned} \quad (28)$$

where we have introduced a causal source term $s = s(t, \mathbf{x})$.

6. Numerical algorithm

6.1. The Fractional Derivative

The computation of the fractional derivative is based on the GL approximation (Podlubny, 1999; Carcione et al., 2002). As we show in the following, the implementation of the distributed orders of differentiation requires a generalization of the backward GL derivative.

The fractional derivative of order z of a function g is

$$\frac{\partial^z g}{\partial t^z} \approx D^z g = \frac{1}{h^z} \sum_{j=0}^J (-1)^j \binom{z}{j} g(t - jh), \quad (29)$$

where h is the time step, and $J = t/h - 1$. The derivation of this expression can be found, for instance, in Carcione et al. (2002). The fractional derivative of g at time t depends on all of the previous values of g . This is the memory property of the fractional derivative, related to field attenuation. The binomial coefficients are negligible for j exceeding an integer J . This allows us to truncate the sum at $j = L$, $L \leq J$, where L is the effective memory length.

6.2. Generalized GL Derivative and Solution Algorithm

Fractional derivatives of order $z \ll 1$ require large memory resources and computational time, because the decay of the binomial coefficients in equation 29 is slow (Carcione et al., 2002; Carcione, 2009), and the effective memory length L is large. We increase

the order of the derivative by applying a time derivative of order m to equation 28. The result is

$$\begin{aligned} D^{m+2}u_1 &= \rho^{-1}\partial_1\tau + D^mf_1, \\ D^{m+2}u_2 &= \rho^{-1}\partial_2\tau + D^mf_2, \\ \tau &= M_0 \int_a^b s(z)D^{m+z}\epsilon \, dz + D^ms, \\ \epsilon &= \partial_1u_1 + \partial_2u_2. \end{aligned} \tag{30}$$

It is enough to take $m = 1$ to have a considerable saving in memory storage compared with $m = 0$. In this case, $\tau = \partial_t\sigma$ is the stress rate.

We discretize equations 30 at $t = nh$ with $m = 1$. Using the notation $u^n = u(nh)$, the left-hand side of the first two equations can be approximated by

$$h^3(D^3u_i)^n = u_i^{n+1} - 3u_i^n + 3u_i^{n-1} - u_i^{n-2}, \quad i = 1, 2, \tag{31}$$

where we have used a right-shifted FD expression for the third derivative.

Using equation 29, the integral containing a GL distributed derivative in the third expression in equation 30 can be approximated as

$$\int_a^b s(z)D^{m+z}g \, dz \approx \frac{1}{h^m} \sum_{j=0}^J C_{mj}g(t - jh), \tag{32}$$

where

$$C_{mj} = (-1)^j \int_a^b \binom{m+z}{j} \frac{s(z)}{h^z} \, dz. \tag{33}$$

Then, from equations 30 and 32 we see that the third expression in equation 30 can be approximated as

$$\tau = \frac{M_0}{h^m} \sum_{j=0}^J C_{mj}\epsilon(t - jh), \tag{34}$$

where

$$C_{mj} = (-1)^j N \int_a^b \binom{m+z}{j} \frac{z^n}{(\omega h)^z} \, dz. \tag{35}$$

for the z^n distribution, and

$$C_{mj} = (-1)^j \sum_{k=1}^n \frac{a_k}{(\omega h)^{z_k}} \binom{m+z_k}{j} \tag{36}$$

for the comb distribution.

Finally, we obtain for $m = 1$,

$$\begin{aligned} u_1^{n+1} &= h^3(\rho^{-1}\partial_1\tau^n) + 3u_1^n - 3u_1^{n-1} + u_1^{n-2}, \\ u_2^{n+1} &= h^3(\rho^{-1}\partial_2\tau^n) + 3u_2^n - 3u_2^{n-1} + u_2^{n-2}, \\ \tau^n &= \frac{M_0}{h} \sum_{j=0}^J C_{1j}\epsilon^{n-j} + D^1s^n, \\ \epsilon^n &= \partial_1u_1^n + \partial_2u_2^n, \end{aligned} \tag{37}$$

which constitute the time stepping method. We do not perform a stability–accuracy analysis of these equations, but in the next section we obtain the FD phase velocity, which compared with the exact phase velocity allows us to evaluate the appropriate value of the time step h to obtain a solution with the desired precision.

The spatial derivatives are calculated with the Fourier method by using the FFT (Carcione, 2007). The Fourier pseudo-spectral method has spectral accuracy for band-limited signals. Then, the results are not affected by spatial numerical dispersion. In the case of inhomogeneous media, the algorithm employs the staggered Fourier method (Carcione, 2009). Since we use Fourier basis functions to compute the spatial derivatives, equation 37 satisfies periodic boundary conditions at the edges of the numerical mesh.

6.3. FD Complex Velocity

The dispersion relation relates the frequency with the wavenumber and allows the calculation of the phase velocity corresponding to each Fourier component. Time discretization implies an approximation of the dispersion relation. Assuming $m = 1$, no body forces, constant material properties, and taking derivatives with respect to x_1 and with respect to x_2 in the first and second expressions in equation 30, respectively, and adding the resulting equations, gives

$$\partial_t^3\epsilon = \frac{1}{\rho} \Delta\tau, \tag{38}$$

where Δ is the Laplacian. Substituting the ansatz $\exp(i\omega t - k_1x - k_2y)$ for ϵ , where k_i are the complex wavenumber components, gives the following FD complex velocity:

$$\bar{v} = \frac{\omega}{k} = c_0(1 + i)\theta \exp(i\theta/2) \sqrt{\frac{\sum_{j=0}^J C_{1j} \exp(-2ij\theta)}{\sin 3\theta - 3 \sin \theta}}, \tag{39}$$

where $\theta = \omega h/2$, $k = \sqrt{k_1^2 + k_2^2}$ and $c_0 = \sqrt{(M_0/\rho)}$. The FD phase velocity, attenuation factor and quality factor are obtained by replacing equation 39 in equations 20 and 26, respectively.

7. Examples

We first consider a material with $M_0 = \rho c_0^2$, where $\rho = 2 \text{ g cm}^{-3}$ and $c_0 = 2 \text{ km s}^{-1}$. The reference frequency is taken $f_0 = \omega_0/(2\pi) = 250 \text{ Hz}$. We assume $a = 0.01$ and $b = 0.02$ (z^n distribution), and $z_1 = 0.01$ and $z_2 = 0.02$ (comb distribution, where $a_1 = 1/3$ and $a_2 = 2/3$). These parameters may describe loss mechanisms which can occur in hydrocarbon reservoirs, where the quality factor of the compressional waves may range between 20 and 50, usually representing high-porosity partially saturated sandstones and limestones. In practice, the parameters are obtained by an optimization

method, by fitting the observed Q factor with the theoretical one. Typical minimization algorithms, such as the Minpack or the BFGS method, can be used.

Figures 1 and 2 show the phase velocity and quality factor for both cases in the frequency range from 0.1 Hz to 10 kHz. The phase velocities for the different values of n coincide at the reference frequency ω_0 . The quality factor is almost constant for practical purposes, while in the case $n = 1$ of Figure 2 (comb distribution), it is constant, since it corresponds to one single order of differentiation $z_2 = 0.02$ (Carcione et al., 2002). The value of ω_0 allows us to determine the desired phase velocity at a given frequency band. The z^n distribution

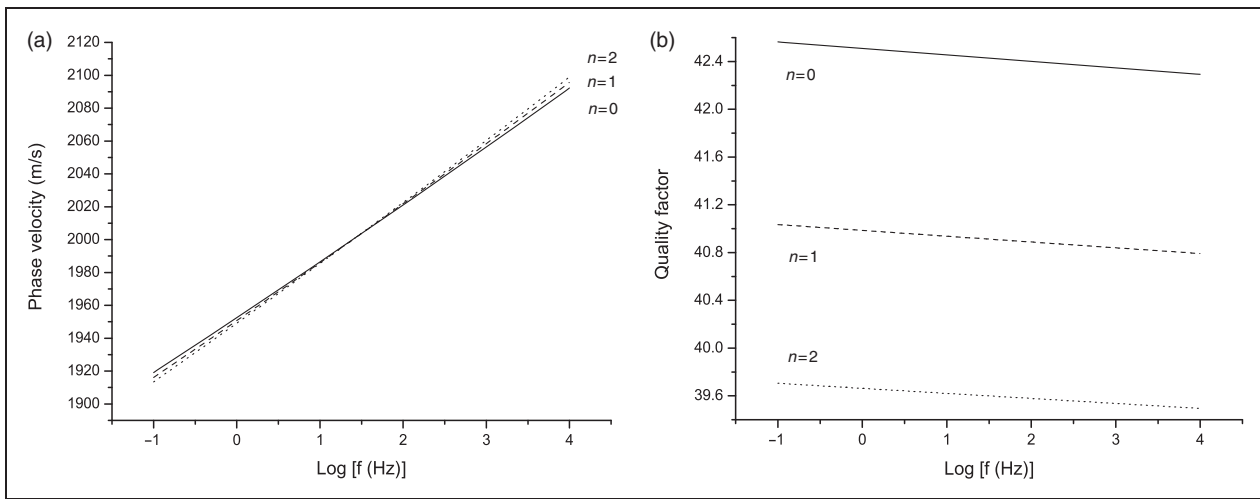


Figure 1. Phase velocity and quality factor for the z^n distribution, with $a = 0.01$ and $b = 0.02$. The solid, dashed and dotted lines correspond to $n = 0, 1$ and 2 , respectively.

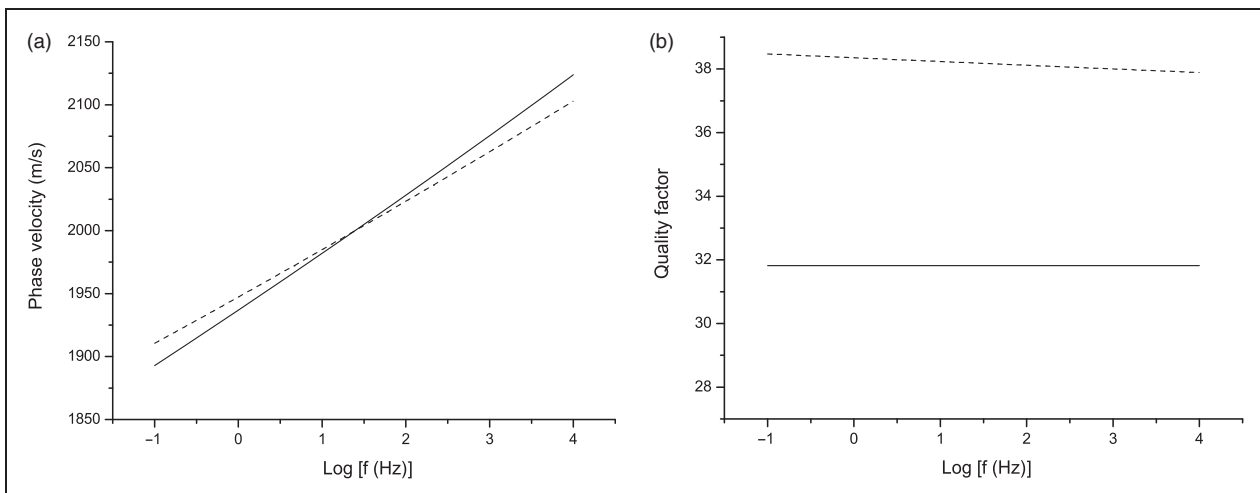


Figure 2. Phase velocity and quality factor for Dirac's comb distribution. The solid and dashed lines correspond to $n = 1$ and 2 , respectively.

allows for a higher resolution to model variations in the phase velocity, due to fine splitting with increasing n (see Figure 1a). However, from a practical point of view, this distribution and the comb distribution are similar.

We evaluate the accuracy of the numerical fractional derivatives for the z^1 distribution by comparing the FD phase velocity and attenuation factor with the exact values. They are shown in Figures 3 and 4 as a function of frequency, for $a = 0.01$, $b = 0.02$, and $a = 0.1$, $b = 0.2$, respectively, where the symbols represent the numerical approximation. The memory length is 120, the reference frequency is $f_0 = 250$ Hz, and the time step is

$h = 0.03$ ms. The velocity dispersion and the attenuation is much stronger in Figure 4. Use of the comb distribution yields a similar agreement.

We now compare the numerical and analytical solutions in homogeneous unbounded media, where the numerical solution is obtained by solving equation 37. The two-dimensional analytical solution is obtained in the appendix. To compute the transient responses, we use as a source a time history of the form:

$$f(t) = \left(a - \frac{1}{2}\right) \exp(-a), \quad a = \left[\frac{\pi(t - t_s)}{t_p}\right]^2, \quad (40)$$

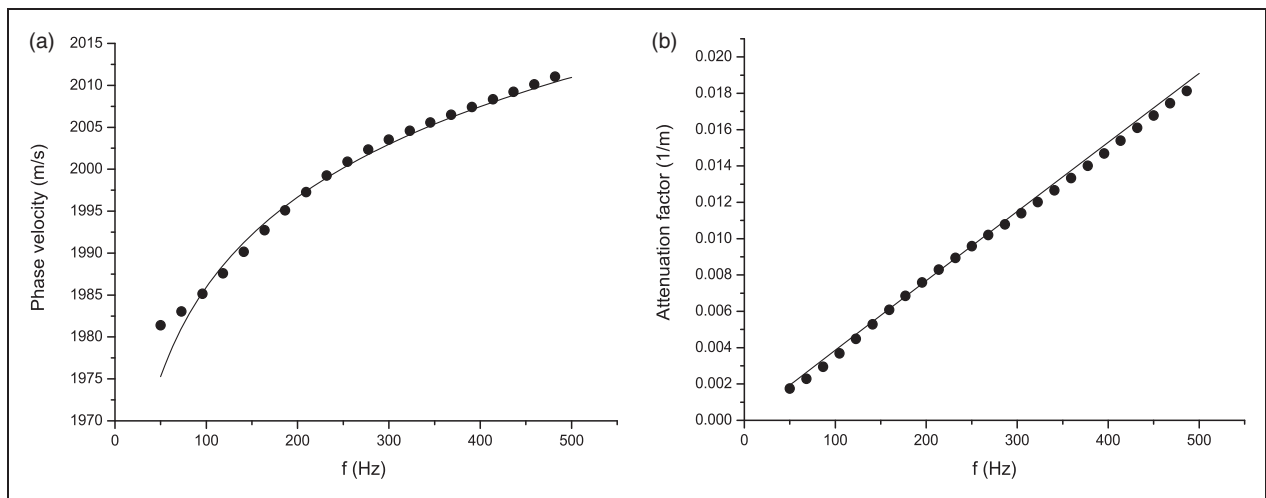


Figure 3. Phase velocity (a) and attenuation factor (b) as a function of frequency. ($a = 0.01$, $b = 0.02$ and $f_0 = \omega_0/(2\pi) = 250$ Hz). The symbols represent the FD approximation.

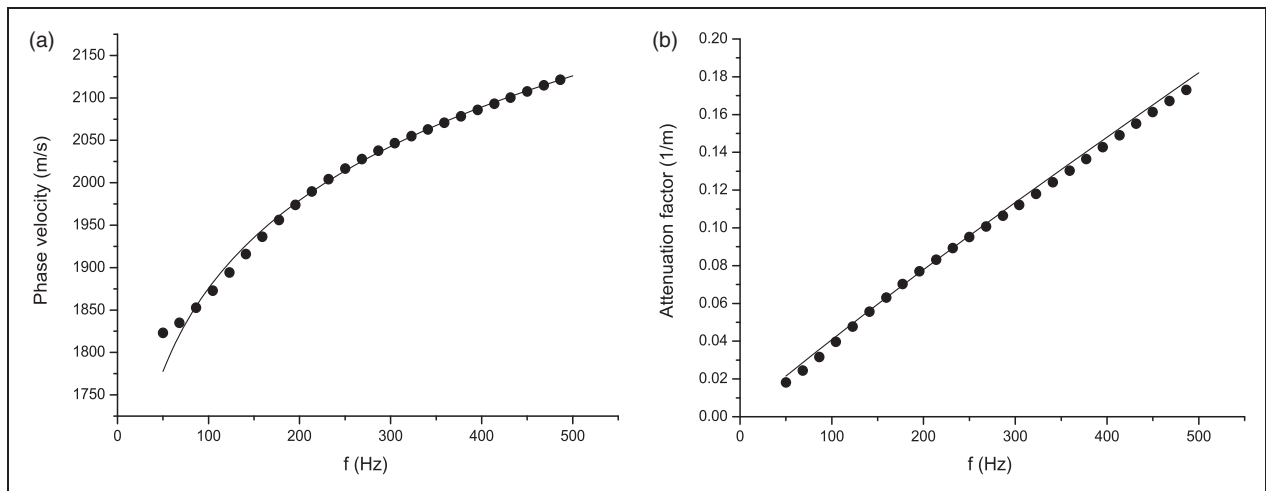


Figure 4. Phase velocity (a) and attenuation factor (b) as a function of frequency. ($a = 0.1$, $b = 0.2$ and $f_0 = \omega_0/(2\pi) = 250$ Hz). The symbols represent the FD approximation.

where t_p is the period of the wave (the distance between the side peaks is $\sqrt{6}t_p/\pi$) and we take $t_s = 1.4t_p$. Its frequency spectrum is

$$F(\omega) = \left(\frac{t_p}{\sqrt{\pi}}\right)\bar{a}\exp(-\bar{a} - i\omega t_s), \quad \bar{a} = \left(\frac{\omega}{\omega_p}\right)^2, \\ \omega_p = \frac{2\pi}{t_p}. \quad (41)$$

The peak frequency is $f_p = 1/t_p$. Figure 5 shows the normalized source spectrum for a peak frequency of 250 Hz.

The medium is discretized on a numerical mesh, with uniform vertical and horizontal grid spacings of 1 m,

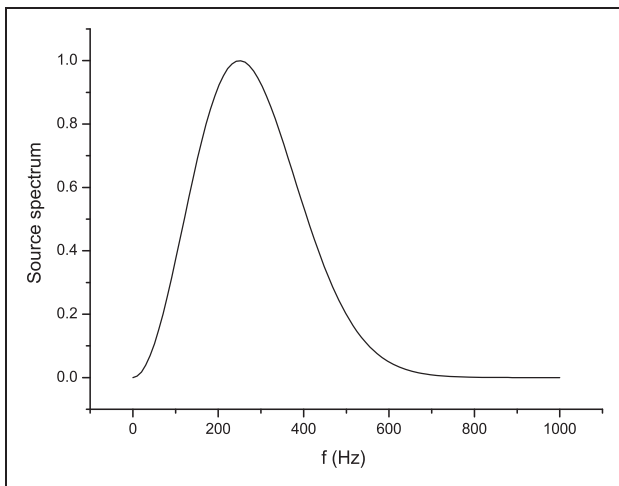


Figure 5. Normalized source spectrum.

and 117×117 grid points. A dilatational source is applied at the center of the mesh and has a peak frequency of 250 Hz. We use a memory length of 120 and a time step $h = 0.03$ ms. Figure 6 compares the analytical and numerical solutions using the z^1 distribution introduced above with a reference frequency $f_0 = 250$ Hz. Figure 6a corresponds to $a = 0.01$ and $b = 0.02$, and Figure 6b to $a = 0.1$ and $b = 0.2$. In Figure 6a the quality factor is approximately equal to 41 (see Figure 1b), while in Figure 6b the quality factor is approximately equal to 4, i.e. there is a strong attenuation. As we can see, the match is perfect in both cases.

The advantage of the numerical algorithm is that it can be used to simulate wave propagation in heterogeneous media, i.e. each point in the mesh can have a different property. In order to illustrate a situation where there is no analytical solution, we consider a plane interface separating two media of dissimilar properties, where the attenuation is described by the z^1 distribution. The upper medium has $a = 0.1$, $b = 0.2$, $\rho = 2 \text{ g cm}^{-3}$ and $c_0 = 2 \text{ km s}^{-1}$, and the lower medium has $a = 0.01$, $b = 0.02$, $\rho = 2.3 \text{ g cm}^{-3}$ and $c_0 = 2.5 \text{ km s}^{-1}$. Owing to the nature of the Fourier method used to compute the spatial derivatives, periodic boundary conditions are satisfied at the edges of the mesh, but the simulation time is such that the wavefield does not reach the boundaries. A snapshot of the stress rate is shown in Figure 7, where the source is indicated by a star and is placed 10 m above the interface. A reflected field from the interface can be appreciated, with strong attenuation above due to the low quality factor of the upper medium (approximately equal to four). The lower medium has much less attenuation and, as a consequence, the refracted field has a high amplitude.

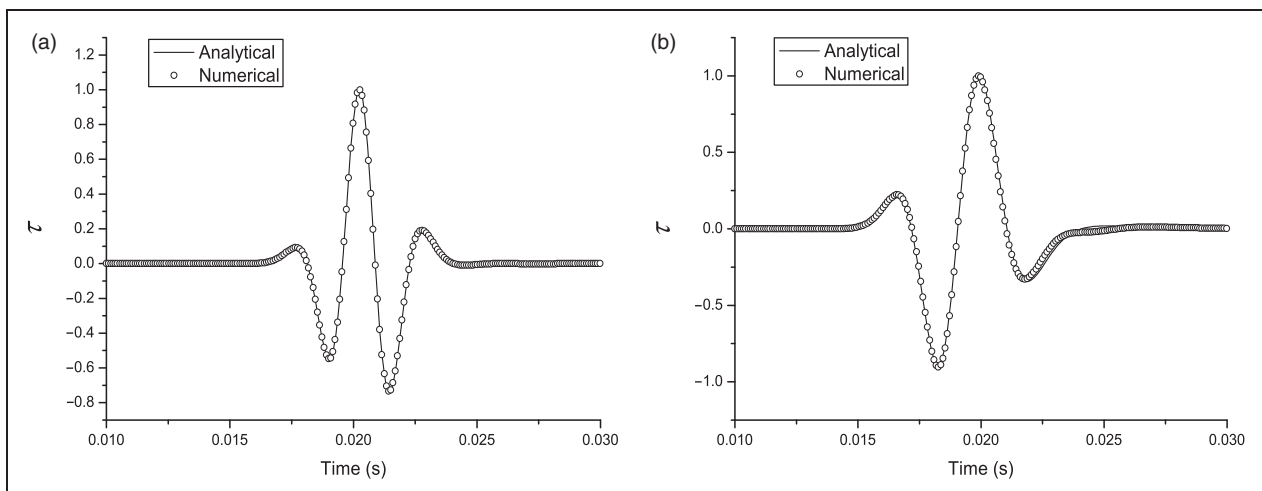


Figure 6. Normalized rate of stress τ . Analytical and numerical solutions corresponding to the z^1 distribution, with (a) $a = 0.01$ and $b = 0.02$ and (b) $a = 0.1$ and $b = 0.2$. The reference frequency f_0 is 250 Hz.

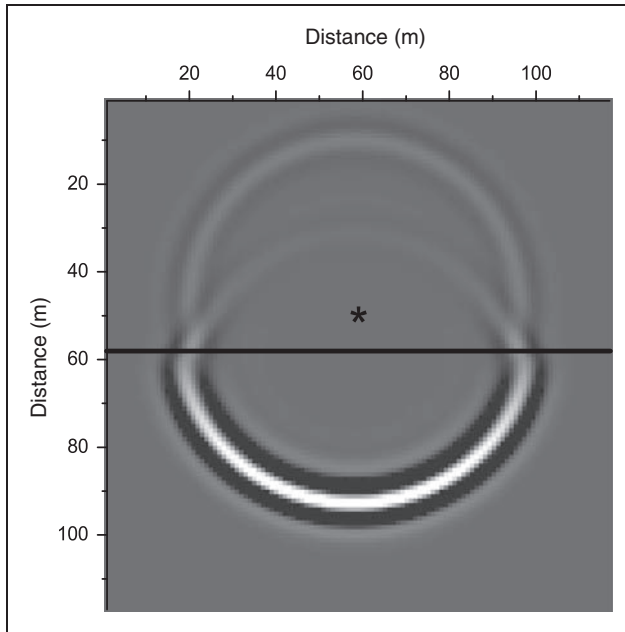


Figure 7. Snapshot of the stress rate τ at 0.024 s. The star indicates the source location and the horizontal line indicates the interface.

8. Conclusions

The wave equation describing attenuation based on fractional time derivatives is generalized to the case when the derivatives are integrated with respect to the order of differentiation. This renders the stress–strain relation more flexible because it includes a variety of memory mechanisms and is more apt to represent the dispersion acting with several different relaxations (e.g. anelastic relaxation mechanisms or spectral lines in the case of dielectric media.).

The power distribution z^n and Dirac's comb function $\sum a_k \delta(z - z_k)$ are considered, where z is the order of differentiation. We obtain an analytical solution in homogeneous media by using the correspondence principle. Moreover, we develop an algorithm for heterogeneous media based on a generalization of the GL approximation of the fractional derivative and the Fourier pseudo-spectral method to compute the spatial derivatives. The numerical solutions show an excellent agreement with the analytical solution. Finally, an heterogeneous model illustrates how the algorithm can handle density, velocity and quality-factor contrasts.

Funding

This research received no specific grant from any funding agency in the public, commercial, or not-for-profit sectors.

Acknowledgment

We thank two anonymous reviewers for useful comments.

References

- Auld BA (1991) *Acoustic Fields and Waves in Solids*. Vol. 1, Malabar, Florida: Robert E. Krieger.
- Bland DR (1960) *The Theory of Linear Viscoelasticity*. Oxford: Pergamon Press.
- Caputo M (1967) Linear models of dissipation whose Q is almost frequency independent-II. *Geophysical Journal of the Royal Astronomical Society* 13: 529–539.
- Caputo M (1995) Mean fractional-order-derivatives. Differential equations and filters. *Annali della Università di Ferrara VII (N. S.)* 41: 73–84.
- Caputo M (2001) Distributed order differential equations modelling dielectric induction and diffusion. *Fractional Calculus and Applied Analysis* 4: 421–442.
- Caputo M and Mainardi F (1971) A new dissipation model based on memory mechanism. *Pure and Applied Geophysics* 91: 134–147.
- Carcione JM (2007) *Wave Fields in Real Media. Theory and Numerical Simulation of Wave Propagation in Anisotropic, Anelastic, Porous and Electromagnetic Media*, 2nd edn revised and extended. Amsterdam: Elsevier Science.
- Carcione JM (2009) Theory and modeling of constant- Q P- and S-waves using fractional time derivatives. *Geophysics* 74: T1–T11.
- Carcione JM, Cavallini F, Mainardi F and Hanyga A (2002) Time-domain seismic modeling of constant Q -wave propagation using fractional derivatives. *Pure and Applied Geophysics* 159: 1719–1736.
- Gorenflo R (1997) Fractional calculus, some numerical methods. In: Carpinteri A and Mainardi F (eds) *Fractals and Fractional Calculus in Continuum Mechanics*. Wien: Springer-Verlag, pp. 277–290.
- Grünwald AK (1867) Über “begrenzte” Derivationen und deren Anwendung. *Zeitschrift für Angewandte Mathematik und Physik* 12: 441–480.
- Hanyga A and Seredyńska M (2003) Power law attenuation in acoustic and isotropic anelastic media. *Geophysical Journal International* 155: 830–838.
- Kjartansson E (1979) Constant Q -wave propagation and attenuation. *Journal of Geophysical Research* 84: 4737–4748.
- Letnikov AV (1868) Theory of differentiation of fractional order. *Matematicheskij Sbornik* 3: 1–68 (in Russian).
- Mainardi F, Mura A, Gorenflo R and Stojanovic M (2007) The two forms of fractional relaxation of distributed order. *Journal of Vibration and Control* 13: 1249–1268.
- Mainardi F, Mura A, Pagnini G and Gorenflo R (2008) Time-fractional diffusion of distributed order. *Journal of Vibration and Control* 14: 1267–1290.
- Mainardi F and Tomirotti M (1997) Seismic pulse propagation with constant Q and stable probability distributions. *Annali di Geofisica* 40: 1311–1328.
- Morse PM and Feshbach H (1953) *Methods of Theoretical Physics*. Vol. II, New York: McGraw-Hill.

Podlubny I (1999) *Fractional Differential Equations*. New York: Academic Press.
 Scott-Blair GW (1949) *Survey of General and Applied Rheology*. London: Pitman.

Appendix: Green’s function and analytical solution

A two-dimensional analytical solution of equation 28 with $m=1$ in a homogeneous medium can easily be obtained. Combining the equations, we have

$$\partial_t^2 \epsilon = \frac{1}{\rho} \Delta(\sigma + s). \tag{42}$$

In the frequency domain, $\sigma = \bar{M}\epsilon = M_0 S\epsilon$, according to equation 9, and equation 42 becomes a Helmholtz equation,

$$\Delta\epsilon + k^2\epsilon = -\frac{1}{\rho v^2} \Delta s = -\frac{1}{M} \Delta s, \quad k = \frac{\omega}{v}, \tag{43}$$

where k is the wavenumber and v is given by equation 19. If v is real, the medium is lossless. The solution to the acoustic (lossless) equation $(\Delta + k^2)G = -\delta\delta(r)$ is the Green function $G = -2iH_0^{(2)}(kr)$, with $v=c_0$, where $H_0^{(2)}$ is the zero-order Hankel function of the second kind (Morse and Feshbach, 1953; Carcione, 2007). More precisely,

$$G(x, y, x_0, y_0, \omega, c_0) = -2i\pi H_0^{(2)}\left(\frac{\omega r}{c_0}\right), \tag{44}$$

where (x_0, y_0) is the source location, and

$$r = \sqrt{(x - x_0)^2 + (y - y_0)^2}. \tag{45}$$

The anelastic solution is obtained by invoking the correspondence principle (Bland, 1960), i.e. by substituting the acoustic velocity c_0 with the complex velocity v . The differential operator Δ/\bar{M} acts on the source in equation 43. Thus, the Green’s function for the strain is

$$G_\epsilon = \frac{1}{\bar{M}} \Delta G. \tag{46}$$

Since $\Delta G = -k^2 G$ away from the source and $\sigma = \bar{M}\epsilon$, the Green’s function for the stress is

$$G_\sigma = \bar{M}G_\epsilon = -k^2 G. \tag{47}$$

We set $G(-\omega) = G^*(\omega)$, where the superscript $*$ denotes complex conjugation. This equation ensures that the inverse Fourier transform of the Green’s function is real. The frequency-domain solution is then given by $\sigma(\omega) = 1/8 G_\sigma(\omega) F(\omega)$, where F is the Fourier transform of the source time history. Since we are solving the dynamical equation with $m=1$, our solution is not σ but the stress rate $\tau = \partial_t \sigma$. Hence,

$$\begin{aligned} \tau(x, y, x_0, y_0, \omega) &= \frac{1}{8} i\omega G_\sigma F \\ &= -\frac{1}{8} i\omega k^2 G(x, y, x_0, y_0, \omega, v) F(\omega). \end{aligned} \tag{48}$$

Because the Hankel function has a singularity at $\omega=0$, we assume $G=0$ for $\omega=0$, an approximation that does not have a significant effect on the solution (note, moreover, that $F(0)=0$). The time-domain solution $\tau(t)$ is obtained by a discrete inverse Fourier transform. We have tacitly assumed that τ and $d\tau/dt$ are zero at time $t=0$.